From Z-Machines to ALMA: (Sub)millimeter Spectroscopy of Galaxies
ASP Conference Series, Vol. TBD, 2006
A. J. Baker, J. Glenn, A. I. Harris, J. G. Mangum, and M. S. Yun, eds.

CO(1–0) Emission from Quasar Host Galaxies Beyond Redshift 4

D. A. Riechers[1], F. Walter[1], C. L. Carilli[2], K. K. Knudsen[1], K. Y. Lo[3], D. J. Benford[4], J. G. Staguhn[4], T. R. Hunter[5], F. Bertoldi[6], C. Henkel[7], K. M. Menten[7], A. Weiss[7], M. S. Yun[8], and N. Z. Scoville[9]

[1]*Max-Planck-Institut für Astronomie, Königstuhl 17, Heidelberg, D-69117, Germany*
[2]*National Radio Astronomy Observatory, PO Box O, Socorro, NM 87801, USA*
[3]*National Radio Astronomy Observatory, 520 Edgemont Road, Charlottesville, VA 22903-2475, USA*
[4]*Laboratory for Observational Cosmology, Code 665, NASA Goddard Space Flight Center, Greenbelt, MD 20771, USA*
[5]*Harvard-Smithsonian Center for Astrophysics, 60 Garden Street, Cambridge, MA 01238, USA*
[6]*Argelander-Institut für Astronomie, Auf dem Hügel 71, Bonn, D-53121, Germany*
[7]*Max-Planck-Institut für Radioastronomie, Auf dem Hügel 69, Bonn, D-53121, Germany*
[8]*Department of Astronomy, University of Massachusetts, 710 North Pleasant Str., Amherst, MA 01003, USA*
[9]*Astronomy Department, California Institute of Technology, Mail Code 105-24, 1200 East California Boulevard, Pasadena, CA 91125, USA*

Abstract. Molecular gas has now been detected in 15 $z > 2$ QSOs through observations of high-J CO transitions using millimeter interferometers. Observations of the CO ground-state transition, CO(1-0), however, have the potential to trace the molecular gas at lower excitations, which may give a better estimate of the total molecular gas content of high-z QSOs. Here we present first $z > 4$ CO(1-0) observations obtained with the NRAO Green Bank Telescope (GBT) and the MPIfR Effelsberg telescope. Utilizing the K band receivers of these two 100m radio telescopes, we detect the CO(1-0) transition in the high-redshift QSOs BR 1202-0725 ($z = 4.7$), PSS J2322+1944 ($z = 4.1$), and APM 08279+5255 ($z = 3.9$). From LVG models based on our observations out to $z = 4.7$, we derive that the CO emission from all observed transitions can be described by a single gas component and that all molecular gas appears to be concentrated in a compact nuclear region. The spectral capabilities of the GBT (1×200 MHz in high-resolution mode, 2×800 MHz in high-bandwidth mode) allow us to cover velocity ranges of up to 22,000 km s^{-1}, or $\Delta z/z = 0.09$ at $z = 4$, which will be imperative for future high-z studies in galaxies with known strong dust continuum, but poorly constrained redshift. This is a first step towards observations with future z machines.

1. Introduction

Over the past decade, 35 galaxies at $z > 2$ have been detected in CO emission (Solomon & Vanden Bout 2005), the 'record holder' being SDSS J1148+5251 at $z = 6.42$ (Walter et al. 2003, 2004; Bertoldi et al. 2003). Studies of the molecular interstellar medium of high–z galaxies are of paramount importance, since it is this medium out of which stars form. An accurate determination of the molecular gas mass (as traced by CO) is a direct indicator of the evolutionary state of a galaxy. Therefore, high–z CO detections imply that large quantities of heavy element enriched gas are already present at these large lookback times; CO observations hence provide direct constraints on the earlier metal enrichment in these galaxies. Due to its low dipole moment ($\mu_{\rm D} = 0.1\,$Debye), CO is excited at lower densities ($n_{\rm crit} \propto 10^2 - 10^3\,{\rm cm}^{-3}$). To excite the higher–$J$ CO transitions, warmer, denser environments are needed ($T_{\rm kin} > 30\,{\rm K}$, $n_{\rm crit} \propto 10^4\,{\rm cm}^{-3}$). Thus, in normal galaxies like the Milky Way, CO is only subthermally excited above $J = 2$. Therefore, only ^{12}CO(J=1→0) traces the full reservoir of molecular gas in those galaxies, while the higher–J transitions only trace the warmer, denser fraction directly involved in star formation (Fixsen et al. 1999, see also Fig. 2). Consequently, the conversion factor, α, to derive molecular (H_2) masses from measured CO luminosities is much better calibrated for the ^{12}CO(J=1→0) line (e.g., Downes & Solomon 1998; Weiss et al. 2001). Observing the ^{12}CO(J=1→0) line also has the advantage that the molecular gas properties of the high–z sources can be *directly* compared to those of nearby (starburst) galaxies, that are predominantly mapped in the ^{12}CO(J=1→0) transition. To date, it is unclear whether the effect of different CO transitions tracing different environments plays a significant role in the extreme sites of vigourous star–formation at high z, as most high–z detections were achieved by observing $J \geq 3$ CO transitions which are typically accessible in the 1–3 mm bands using millimeter–wave telescopes (e.g., IRAM PdBI and 30m, OVRO). In addition, high–z source selection via ^{12}CO(J=1→0) can also significantly reduce the current selection bias introduced by initial detection of high–J millimeter CO lines.

These are the main motivations for observing the CO ground–state transition. Due to the faintness of the line and the bandwidth limitations (requiring very accurate redshifts) of current radio telescopes, such $z > 2$ ^{12}CO(J=1→0) detections yet exist for only two QSOs and two radio galaxies; they were obtained with the NRAO Very Large Array (VLA; Papadopoulos et al. 2001; Carilli et al. 2002a; Greve et al. 2004) and the Australia Telescope Compact Array (ATCA; Klamer et al. 2005). Due to the bandwidth limitations of the VLA, obtaining better constraints on the spectral line shape and total flux density of the ^{12}CO(J=1→0) transition is desirable even for already detected sources. Today's largest single dish telescopes, such as the NRAO Green Bank Telescope (GBT)[1] and the MPIfR Effelsberg telescope[2], can eliminate some of those issues due to their larger spectral bandwidths.

---

[1]The GBT is a facility of the National Radio Astronomy Observatory, operated by Associated Universities, Inc., under a cooperative agreement with the National Science Foundation.

[2]The Effelsberg telescope is a facility of the Max-Planck-Gesellschaft (MPG), operated by the Max-Planck-Institut für Radioastronomie (MPIfR).

2. Observations

2.1. GBT

The sources in our study are the three CO–brightest high–redshift QSOs that can currently be observed in the ^{12}CO(J=1→0) transition. Observations towards BR 1202-0725, PSS J2322+1944, and APM 08279+5255 were carried out with the GBT in ON–OFF position switching mode between October 2004 and April 2005 with a total observing time of 89.5 hours. As the ^{12}CO(J=1→0) transition at 115.2712 GHz is redshifted into the radio K band for all three targets (see Table 1), the dual–beam, dual–polarization 18–26 GHz receiver was used for all observations. The beam size of the GBT at our observing frequencies is $\sim$34″ ($\sim$240 kpc at $z \simeq 4$), i.e., much larger than our targets. The pointing accuracy, was typically $\sim$1″. Two different spectrometer setups were used. The first mode features two intermediate frequencies (IFs) with a bandwidth of 800 MHz ($\sim$11,000 km s^{-1} at our observing frequencies) and 2048 channels each, resulting in a spectral resolution of 391 kHz ($\sim$5 km s^{-1}). The second mode has one IF with 200 MHz ($\sim$2,700 km s^{-1}) and 16384 channels, resulting in a spectral resolution of 12 kHz ($\sim$0.16 km s^{-1}). The weather was excellent for the winter nights with typical zenith system temperatures of $T_{\rm sys} = 22 - 35$ K on $T_{\rm A}^{\star}$ scale (except for April 19 and 20: typically $T_{\rm sys} = 50 - 60$ K).

While GBTIDL has now become the standard data reduction package, many routines exist to reduce GBT data, written both for aips++ (standard 'calib' with significant differences between 2004 and 2005 versions, a specialized version programmed by Bob Garwood, and a different routine written by Ron Maddalena) and in IDL (GBTIDL and Glen Langston's routines). While results produced by these routines are similar in general, there are small differences which help to understand possible problems with single datasets. A polynomial baseline of order 1 was subtracted from the final PSS J2322+1944 spectrum to remove continuum fluxes and atmospheric/instrumental effects. For BR 1202-0725 and APM 08279+5255, polynomials of order 2 have been used to remove a very wide ($\gg$100 MHz, i.e., much broader than the width of the CO line) 'bending' of the baselines. In addition to simple ON-OFF combinations and subtraction of low–order polynomial spectral baselines, we followed the scheme proposed by Vanden Bout et al. (2004) for reconstructing the temporal baseline variations. However, this did not improve our final results.

2.2. Effelsberg

Observations were carried out towards BR 1202-0725 and PSS J2322+1944 in January and February 2003 with a total observing time of $\sim$40 hours. At 40″ beam size, the pointing accuracy was better than 10″. Using a dual channel HEMT receiver, we observed in beam switching mode with a beam throw of 2′ and a switching frequency of $\sim$1 Hz. The autocorrelator backend was split into eight bands of 160 MHz bandwidth and 128 channels each (channel spacings of 1.25 MHz, or $\sim$16 km s^{-1}) that could individually be shifted in frequency by up to $\pm$250 MHz relative to the recessional velocity of the targets. Typical $T_{\rm sys}$ in this run were 47 K (BR 1202-0725) and 60 K (PSS J2322+1944) on $T_{\rm A}^{\star}$ scale after combination of both orthogonal polarizations. All spectral baselines are of excellent quality; only first order polynomial baselines had to be subtracted.

3. Results

3.1. BR 1202-0725

BR 1202-0725 was observed for 20 hours (on–source) with the GBT using both setups described in Sect. 2.1. The final smoothed ^{12}CO(J=1→0) spectrum for this source is shown in the top left panel of Fig. 1 combining observations with both 200 MHz and 800 MHz bandwidth. Gaussian fitting to the line profile results in a peak flux density of 0.36 ± 0.07 mJy and a FWHM of 329 ± 47 km s^{-1}. The integrated ^{12}CO(J=1→0) line flux is 0.124 ± 0.025 Jy km s^{-1}. This agrees well with the extrapolated value of 0.123 ± 0.013 Jy km s^{-1} derived from the ^{12}CO(J=2→1) flux (Carilli et al. 2002b) under assumption of fully thermalized and optically thick CO emission (see also discussion in Sect. 4.1). The width of the ^{12}CO(J=1→0) line is consistent within the error bars with an average of the higher–J transitions in the literature (∼ 290 km s^{-1}). The derived redshift of 4.6938 ± 0.0006 is in excellent agreement with the ^{12}CO(J=5→4) redshift (Omont et al. 1996, northern and southern components combined). This source remains unresolved in our measurements, all line parameters are in good agreement with the higher–J lines adding up both components.

An effective total of 8 hours was spent on–source with Effelsberg. The final spectrum is shown in the top right panel of Fig. 1. The line is detected at moderate signal–to–noise, resulting in a linewidth of 560 ± 210 km s^{-1}, which is consistent (within the uncertainties) with the GBT result. The line peak flux of 0.39 ± 0.16 mJy is in good agreement with the GBT measurement, resulting in an integrated line flux of 0.23 ± 0.09 Jy km s^{-1}. The redshift of 4.6888 ± 0.0015 is slightly offset relative to the Omont et al. (1996) ^{12}CO(J=5→4) redshift with both components combined (by 190 ± 80 km s^{-1}), which we attribute to the moderate signal–to–noise of this measurement.

3.2. PSS J2322+1944

PSS J2322+1944 was observed for 15 hours (on–source) with the GBT using only the high spectral resolution 200 MHz bandwidth setup. The resulting spectrum for the ^{12}CO(J=1→0) line is presented in the middle left panel of Fig. 1. From Gaussian fitting, the peak line flux density is found to be 0.72 ± 0.16 mJy, the line FWHM is 202 ± 31 km s^{-1}, and the integrated line flux is 0.154 ± 0.041 Jy km s^{-1}. These values are in good agreement with the ^{12}CO(J=1→0) detection of Carilli et al. (2002a; $S_\nu = 0.89 \pm 0.22$ mJy, $\Delta V_{\rm FWHM} = 200 \pm 70$ km s^{-1}, $I = 0.19 \pm 0.08$ Jy km s^{-1}), though results for the higher–J CO transitions indicate a larger linewidth ($\Delta V_{\rm FWHM} > 250$ km s^{-1}). Our derived redshift of 4.1173 ± 0.0005 deviates from the previously found ^{12}CO(J=1→0) redshift of 4.1192 ± 0.0004 by 0.0019 (or 111 km s^{-1}), which corresponds to 4σ. We attribute this discrepancy to the moderate signal–to–noise of our observations and problems with baseline instabilities in the nights with higher $T_{\rm sys}$.

An effective total of 8 hours was spent on–source with Effelsberg. The final spectrum is shown in the middle right panel of Fig. 1. The observed ^{12}CO(J=1→0) line peak flux density of 1.27 ± 0.41 mJy and the linewidth of 184 ± 40 km s^{-1} are in agreement with Carilli et al. (2002a) and the GBT results within the errors, leading to an integrated line flux of 0.29 ± 0.06 Jy km s^{-1}. The redshift of 4.1185 ± 0.0003 agrees well with previous observations.

3.3. APM 08279+5255

APM 08279+5255 was observed for 22 hours (on–source) with the GBT using both the 200 MHz and 800 MHz bandwidth setups. Due to significantly better spectral baselines, we only show the results obtained with the wide 800 MHz bandwidth setup in the bottom panel of Fig. 1 (covering ∼8,000 km s^{-1}).

We derive a ^{12}CO(J=1→0) peak flux of 0.26 ± 0.08 mJy and an FWHM of 556 ± 55 km s^{-1} from our Gaussian fit. This results in an integrated line flux of 0.152 ± 0.045 Jy km s^{-1}, which is in excellent agreement with the value of 0.15 ± 0.045 Jy km s^{-1} found by Papadopoulos et al. (2001) for the central ∼ 1″ (corresponding to ∼7.2 kpc at the source redshift) and consistent with results of Lewis et al. (2002) within the error bars. Also, the derived FWHM velocity width is in agreement with single–dish observations of the ^{12}CO(J=6→5), ^{12}CO(J=10→9), and ^{12}CO(J=11→10) transitions obtained with the IRAM 30 m telescope (Weiss et al. 2006, in prep.) and IRAM Plateau de Bure interferometer observations of the ^{12}CO(J=4→3) transition (480 ± 35 km s^{-1}, Downes et al. 1999), as is our derived ^{12}CO(J=1→0) redshift of 3.9122 ± 0.0007.

4. LVG analysis

To investigate what fraction of the ^{12}CO(J=1→0) emission in our target QSOs is associated with the molecular gas reservoirs detected in the higher–J CO transitions, we compared the observations with spherical, one–component large velocity gradient models (LVG). All these LVG calculations use the collision rates from Flower & Pineau des Forets (2001) with an ortho/para H_2 ratio of 3 and a CO abundance per velocity gradient of $[\mathrm{CO}]/\nabla v = 1 \times 10^{-5}\,\mathrm{pc}\,(\mathrm{km\,s^{-1}})^{-1}$ (Weiss et al. 2005). Models were fitted to those lines *above* the ^{12}CO(J=1→0) transition from the literature for each source. As an example, Fig. 2 shows data of all transitions and three representative models for BR 1202-0725. An apparent degeneracy exists between the kinetic gas temperature T_{kin} and density $\rho_{\mathrm{gas}}(H_2)$, the two main free parameters in our study, but the LVG predicted ^{12}CO(J=1→0) flux of the different models based on the $J > 1$ CO transitions is fairly well constrained by the solutions. Most of our calculated models suggest that the CO emission is close to thermalized up to the ^{12}CO(J=4→3) transition and optically thick ($\tau \simeq 5$), which implies that the LVG predicted ^{12}CO(J=1→0) line fluxes are similar to those we would derive by assuming a ν^2 scaling of the line flux densities from the mid–J CO transitions.

Our observations and models are in agreement with the assertion that *all* observed ^{12}CO(J=1→0) flux density is associated with the highly excited molecular gas seen in the high–J CO lines. We thus find no evidence for an additional luminous, more extended low surface brightness gas component surrounding the central region of our target QSOs, in contrast to what has been suggested previously for APM 08279+5255 (Papadopoulos et al. 2001). Given the accuracy of our measurements, we conclude that at most 20-30% of the ^{12}CO(J=1→0) luminosity may be associated with such a diffuse component. However, if the L'_{CO} to $M_{\mathrm{gas}}(H_2)$ conversion factor, α, for the extended component were Galactic rather than starburst–like, a higher H_2 mass may be hidden in such an extended component. In any case, the fact that single component models fit the line strengths of all CO transitions in all three sources observed implies that calibrations done for

^{12}CO(J=1→0) at low z can also directly be applied to observations of higher–J CO transitions for our target QSOs.

5. Summary

We have detected ^{12}CO(J=1→0) emission towards three QSOs at redshifts $3.9 < z < 4.7$ with the GBT and the MPIfR Effelsberg telescope. We find that ^{12}CO(J=1→0) fluxes predicted by one–component LVG models are in excellent agreement with our observations for all sources. Considering our modeling results, the CO emission appears to be thermalized up to the $J = 4 \rightarrow 3$ transition, and all CO emission is described very well by a single gas component, where all molecular gas is concentrated in a compact nuclear region.

Since we did not detect a significant low–excitation molecular gas component in any of the high–z QSOs, these systems appear to have a high fraction of dense, warm gas that is associated with star formation. In this respect, they are similar to low–z ULIRGs (Gao & Solomon 2004).

The observations presented here demonstrate the feasibility to detect high–z CO with 100 m single–dish radio telescopes equipped with state–of–the–art receivers. The broad spectral bandwidth and resolution of the GBT allows us to study molecular lines in great detail already today, but will also be significantly improved once the $K_{\rm A}$ band receiver at 26–40 GHz and its z-machine, the *Zpectrometer*, become fully operational. Therefore, the unique spectral capabilities of the GBT will be imperative for future CO studies in galaxies with known strong dust continuum, but poorly restricted redshift.

Acknowledgments. D. A. R. acknowledges support from the Deutsche Forschungsgemeinschaft (DFG) Priority Programme 1177. C. C. would like to acknowledge support from the Max-Planck-Forschungspreis.

References

Bertoldi, F., Cox, P., Neri, R., et al. 2003, A&A, 409, L47
Carilli, C. L., Cox, P., Bertoldi, F., et al. 2002a, ApJ, 575, 145
Carilli, C. L., Kohno, K., Kawabe, R., et al. 2002b, AJ, 123, 1838
Downes, D., & Solomon, P. M. 1998, ApJ, 507, 615
Downes, D., Neri, R., Wiklind, T., et al. 1999, ApJ, 513, L1
Fixsen, D. J., Bennett, C. L., & Mather, J. C. 1999, ApJ, 526, 207
Flower, D. R., & Pineau des Forets, G. 2001, MNRAS, 323, 672
Gao, Y., & Solomon, P. M. 2004, ApJ, 606, 271
Greve, T. R., Ivison, R. J., & Papadopoulos, P. P. 2004, A&A, 419, 99
Klamer, I. J., Ekers, R. D., Sadler, E. M., et al. 2005, ApJ, 621, L1
Lewis, G. F., Carilli, C., Papadopoulos, P., & Ivison, R. J. 2002, MNRAS, 330, L15
Omont, A., Petitjean, P., Guilloteau, S., et al. 1996, Nature, 382, 428
Papadopoulos, P., Ivison, R., Carilli, C. L., & Lewis, G. 2001, Nature, 409, 58
Solomon, P. M., & Vanden Bout, P. A. 2005, ARA&A, 43, 677
Vanden Bout, P. A., Solomon, P. M., & Maddalena, R. J. 2004, ApJ, 614, L97
Walter, F., Bertoldi, F., Carilli, C. L., et al. 2003, Nature, 424, 406
Walter, F., Carilli, C., Bertoldi, F., et al. 2004, ApJ, 615, L17
Weiss, A., Neininger, N., Hüttemeister, S., & Klein, U. 2001, A&A, 365, 271
Weiss, A., Walter, F., & Scoville, N. Z. 2005, A&A, 438, 533

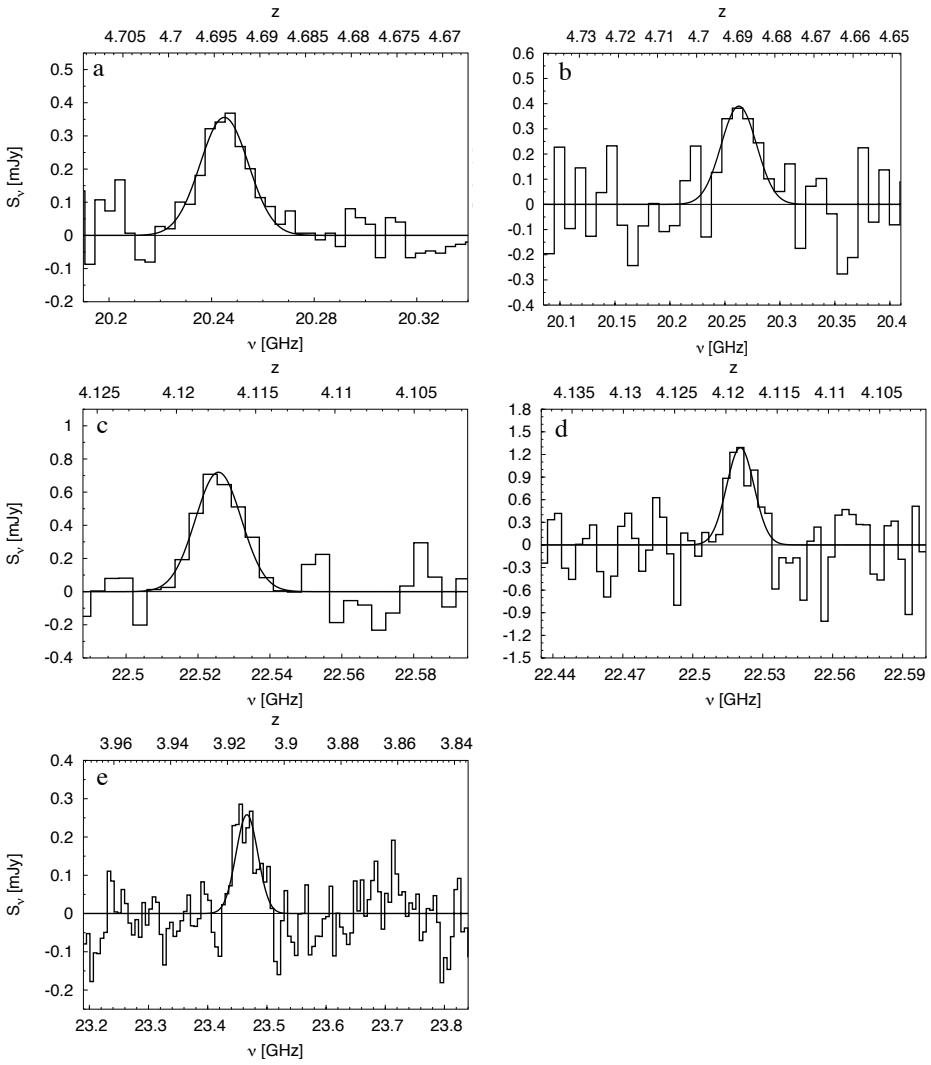

Figure 1. GBT (*left*) and Effelsberg (*right*) spectra of ^{12}CO(J=1→0) emission from BR 1202-0725 (**a**,**b**), PSS J2322+1944 (**c**,**d**), and APM 08279+5255 (**e**). The black line shows a Gaussian fit to the data with parameters given in Table 1. The original spectra have been smoothed, and the resolution and rms per channel are **a**: 3.91 MHz (58 km s^{-1}) and ∼70 μJy; **b**: 9.52 MHz (141 km s^{-1})and ∼160 μJy; **c**: 3.91 MHz (52 km s^{-1}) and ∼160 μJy; **d**: 3.01 MHz (40 km s^{-1}) and ∼410 μJy; and **e**: 5.86 MHz (75 km s^{-1}) and ∼80 μJy.

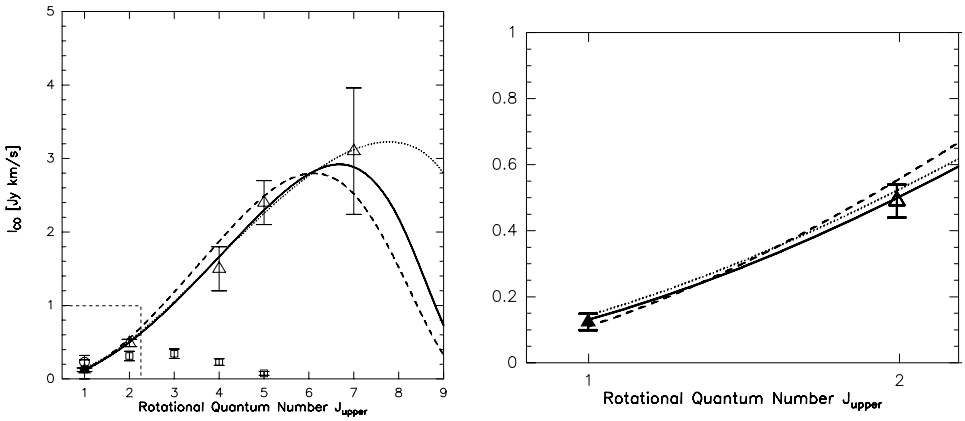

Figure 2. CO ladder and LVG models (based on all $J > 1$ transitions) for BR 1202-0725. The left panel shows the full dataset, while the right panel shows a zoomed–in version of the $J = 2$, $J = 1$ region (as indicated by the dashed box in the left panel). Open circles are the Effelsberg data, filled triangles are the GBT data. Data for the higher–J CO transitions (open triangles) are taken from the literature. For comparison, we also show data for the inner disk of the Milky Way (open squares, Fixsen et al. 1999), normalized to the ^{12}CO(J=1→0) flux of BR 1202-0725. The kinetic temperature $T_{\rm kin}$ and gas density $\rho_{\rm gas}(H_2)$ are treated as free parameters in this study. Three representative models are shown: Model 1 (solid line) assumes $T_{\rm kin} = 65\,{\rm K}$ and $\rho_{\rm gas}(H_2) = 10^{4.3}\,{\rm cm}^{-3}$, and gives the overall best fit to all transitions. Model 2 assumes $T_{\rm kin} = 100\,{\rm K}$ and $\rho_{\rm gas}(H_2) = 10^{4.0}\,{\rm cm}^{-3}$, while model 3 assumes $T_{\rm kin} = 50\,{\rm K}$ and $\rho_{\rm gas}(H_2) = 10^{4.9}\,{\rm cm}^{-3}$.

Table 1. Observed line parameters for our ^{12}CO(J=1→0) detections.

Source	z	$\nu_{\rm obs}$ [GHz]	S_ν[a] [mJy]	$\Delta V_{\rm FWHM}$ [km s^{-1}]	I [Jy km s^{-1}]	Telescope
BR 1202-0725	4.6938 ± 0.0006	20.2450	0.36 ± 0.07	329 ± 47	0.124 ± 0.025	GBT
PSS J2322+1944	4.1173 ± 0.0005	22.5257	0.72 ± 0.16	202 ± 31	0.154 ± 0.041	GBT
APM 08279+5255	3.9122 ± 0.0007	23.4663	0.26 ± 0.08	556 ± 55	0.152 ± 0.045	GBT
BR 1202-0725	4.6888 ± 0.0015	20.2627	0.39 ± 0.16	560 ± 210	0.23 ± 0.09	Effelsberg
PSS J2322+1944	4.1185 ± 0.0003	22.5204	1.27 ± 0.41	184 ± 40	0.29 ± 0.06	Effelsberg

[a] rms values are given for a 58/52/75/141/40 km s^{-1} channel (in the given source order).